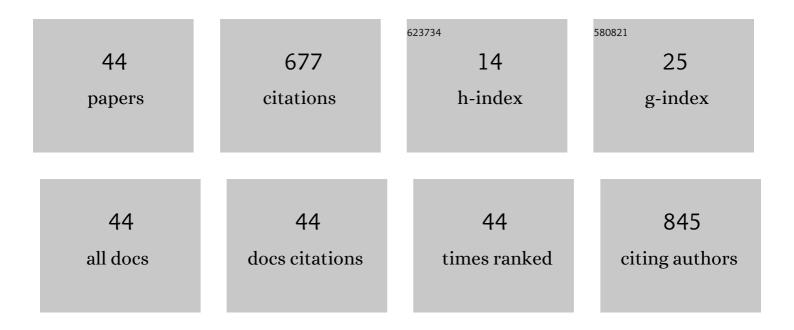


List of Publications by Year in descending order

Source: https://exaly.com/author-pdf/7149459/publications.pdf Version: 2024-02-01



WENRO

#	Article	IF	CITATIONS
1	Exploiting Memristive BiFeO ₃ Bilayer Structures for Compact Sequential Logics. Advanced Functional Materials, 2014, 24, 3357-3365.	14.9	116
2	A synaptic memristor based on two-dimensional layered WSe ₂ nanosheets with short- and long-term plasticity. Nanoscale, 2021, 13, 6654-6660.	5.6	51
3	Forming-Free Resistive Switching in Multiferroic BiFeO ₃ thin Films with Enhanced Nanoscale Shunts. ACS Applied Materials & Interfaces, 2013, 5, 12764-12771.	8.0	50
4	PMN-PT/PVDF Nanocomposite for High Output Nanogenerator Applications. Nanomaterials, 2016, 6, 67.	4.1	34
5	Rectifying filamentary resistive switching in ion-exfoliated LiNbO3 thin films. Applied Physics Letters, 2016, 108, .	3.3	30
6	Surface modifications of crystal-ion-sliced LiNbO3 thin films by low energy ion irradiations. Applied Surface Science, 2018, 434, 669-673.	6.1	28
7	The thin film bulk acoustic wave resonator based on single-crystalline 43â—‹Y-cut lithium niobate thin films. AIP Advances, 2020, 10, .	1.3	26
8	Mo/Ti multilayer Bragg reflector for LiNbO3 film bulk acoustic wave resonators. Journal of Applied Physics, 2020, 128, .	2.5	23
9	Highly heterogeneous epitaxy of flexoelectric BaTiO3-δ membrane on Ge. Nature Communications, 2022, 13, .	12.8	22
10	Quick response PZT/P(VDF-TrFE) composite film pyroelectric infrared sensor with patterned polyimide thermal isolation layer. Infrared Physics and Technology, 2014, 66, 34-38.	2.9	21
11	Ferroelectric and flexible barrier resistive switching of epitaxial BiFeO3 films studied by temperature-dependent current and capacitance spectroscopy. Journal of Materials Science: Materials in Electronics, 2016, 27, 7927-7932.	2.2	16
12	Ar+ ions irradiation induced memristive behavior and neuromorphic computing in monolithic LiNbO3 thin films. Applied Surface Science, 2019, 484, 751-758.	6.1	16
13	Monolithic pyroelectric infrared detectors using SiO2 aerogel thin films. Sensors and Actuators A: Physical, 2015, 228, 69-74.	4.1	15
14	Forming free resistive switching in Au/TiO2/Pt stack structure. Thin Solid Films, 2016, 617, 63-66.	1.8	15
15	Lead free KNN/P(VDF-TrFE) 0–3 pyroelectric composite films and its infrared sensor. Infrared Physics and Technology, 2017, 80, 100-104.	2.9	15
16	Infrared detector based on crystal ion sliced LiNbO3 single-crystal film with BCB bonding and thermal insulating layer. Microelectronic Engineering, 2019, 213, 1-5.	2.4	15
17	Reliable resistive switching and synaptic plasticity in Ar+-irradiated single-crystalline LiNbO3 memristor. Applied Surface Science, 2022, 596, 153653.	6.1	15
18	Fabrication of Y128- and Y36-cut lithium niobate single-crystalline thin films by crystal-ion-slicing technique. Japanese Journal of Applied Physics, 2018, 57, 04FK05.	1.5	14

Wenbo

#	Article	IF	CITATIONS
19	Fabrication of lead selenide thin film photodiode for near-infrared detection via O2-plasma treatment. Journal of Alloys and Compounds, 2018, 753, 6-10.	5.5	12
20	A Comprehensive Study of a Micro-Channel Heat Sink Using Integrated Thin-Film Temperature Sensors. Sensors, 2018, 18, 299.	3.8	12
21	Lithium niobate single crystal thin film resonator with benzocyclobutene as a reflective layer. Japanese Journal of Applied Physics, 2020, 59, 016502.	1.5	12
22	A Low Temperature Drifting Acoustic Wave Pressure Sensor with an Integrated Vacuum Cavity for Absolute Pressure Sensing. Sensors, 2020, 20, 1788.	3.8	12
23	A Solidly Mounted Resonator Fabricated by LiNbO ₃ Single-Crystalline Film on Flexible Polyimide Substrate. IEEE Transactions on Ultrasonics, Ferroelectrics, and Frequency Control, 2021, 68, 2585-2589.	3.0	12
24	Voltage-programmable negative differential resistance in memristor of single-crystalline lithium niobate thin film. Applied Physics Letters, 2022, 120, .	3.3	11
25	High specific detectivity infrared detector using crystal ion slicing transferred LiTaO3 single-crystal thin films. Sensors and Actuators A: Physical, 2019, 300, 111650.	4.1	10
26	Resistive Switching Effects of Crystalâ€lonâ€6licing Fabricated LiNbO ₃ Single Crystalline Thin Film on Flexible Polyimide Substrate. Advanced Electronic Materials, 2021, 7, 2100301.	5.1	10
27	An infrared pyroelectric detector improved by cool isostatic pressing with cup-shaped PZT thick film on silicon substrate. Infrared Physics and Technology, 2013, 61, 313-318.	2.9	8
28	Investigation of the Temperature Fluctuation of Single-Phase Fluid Based Microchannel Heat Sink. Sensors, 2018, 18, 1498.	3.8	8
29	BAW Resonator with an Optimized SiO ₂ /Ta ₂ O ₅ Reflector for 5G Applications. ACS Omega, 2022, 7, 20994-20999.	3.5	8
30	Effects of Ar+ irradiation on the performance of memristor based on single-crystalline LiNbO3 thin film. Journal of Materials Science: Materials in Electronics, 2021, 32, 20817-20826.	2.2	7
31	Surfactant-Assisted Hydrothermal Synthesis of PMN-PT Nanorods. Nanoscale Research Letters, 2016, 11, 49.	5.7	6
32	Observation of nonvolatile resistive switching behaviors in 2D layered InSe nanosheets through controllable oxidation. Applied Physics Letters, 2021, 119, .	3.3	6
33	Compliance-current-modulated resistive switching with multi-level resistance states in single-crystalline LiNbO3 thin film. Solid State Ionics, 2019, 334, 1-4.	2.7	4
34	A simple implement of submicron meter RRAM array based on porous SiO 2 film with uniform and large pores. Vacuum, 2016, 132, 119-122.	3.5	3
35	Numerical and Experimental Study of Valve-Less Micropump Using Dynamic Multiphysics Model. , 2018, ,		3
36	Fabrication of large-scale flexible silicon membrane by crystal-ion-slicing technique using BCB bonding layer. Applied Physics A: Materials Science and Processing, 2021, 127, 1.	2.3	3

Wenbo

#	Article	IF	CITATIONS
37	Effects of helium implantation fluence on the crystal-ion-slicing fabrication of Y-cut lithium niobate film. Materials Express, 2021, 11, 717-723.	0.5	2
38	Effects of rapid thermal annealing parameters on crystal ion slicing-fabricated LiTaO3 thin film. Applied Physics A: Materials Science and Processing, 2021, 127, 1.	2.3	2
39	Microchannel Heat Sink with Enhanced Heat Transfer Performance by Laser Process. , 2018, , .		1
40	Ultra-high Efficient Integrated Microchannel Cooling for Multi-unit Microsystems. , 2019, , .		1
41	Oxygen vacancy induced phase and conductivity transition of epitaxial BaTiO3â ^{^ĵ^} films directly grown on Ge (001) without surface passivation. Journal of Applied Physics, 2021, 129, 045302.	2.5	1
42	Ion Implantation Caused Defects and Their Effects on LiTaO ₃ Crystal Exfoliation. Physica Status Solidi (A) Applications and Materials Science, 2022, 219, .	1.8	1
43	Investigation of Temperature Fluctuation Resulted in Dissolved Gas for Single-Phase Microchannel Heat Sink. , 2018, , .		0
44	Investigation of Temperature Fluctuation Resulted in Dissolved Gas for Single-Phase Microchannel Heat Sink. , 2018, , .		0